ESC European Society of Cardiology

Cardiovascular Research (2022) **118**, 1728–1741
https://doi.org/10.1093/cvr/cvab177

Treatment of atrial fibrillation with doxapram: TASK-1 potassium channel inhibition as a novel pharmacological strategy

Felix Wiedmann [1,2,3], Christoph Beyersdorf[1,3], Xiao-Bo Zhou[2,4], Manuel Kraft[1,2,3], Amelie Paasche[1,3], Natasa Jávorszky[1,3], Susanne Rinné[5], Henry Sutanto [6], Antonius Büscher[1,2,3], Kathrin I. Foerster [7], Antje Blank [7], Ibrahim El-Battrawy[2,4], Xin Li[4], Siegfried Lang[2,4], Ursula Tochtermann[8], Jamila Kremer[8], Rawa Arif[8], Matthias Karck[8], Niels Decher[5], Gunther van Loon[9], Ibrahim Akin[2,4], Martin Borggrefe[2,4], Stefan Kallenberger [10,11], Jordi Heijman [6], Walter E. Haefeli [7], Hugo A. Katus[1,2,3], and Constanze Schmidt [1,2,3]*

[1]Department of Cardiology, University Hospital Heidelberg, Im Neuenheimer Feld 410, 69120 Heidelberg, Germany; [2]Partner site Heidelberg /Mannheim, DZHK (German Center for Cardiovascular Research), Potsdamer Straße 58, 10785 Berlin, Germany; [3]HCR, Heidelberg Center for Heart Rhythm Disorders, University Hospital Heidelberg, Im Neuenheimer Feld 410, 69120 Heidelberg, Germany; [4]First Department of Medicine, University Medical Center Mannheim, Theodor-Kutzer-Ufer 1-3, 68167 Mannheim, Germany; [5]Institute for Physiology and Pathophysiology, Vegetative Physiology and Marburg Center for Mind, Brain and Behavior MCMBB, University of Marburg, Deutschhausstrasse 1-2, 35037 Marburg, Germany; [6]Cardiovascular Research Institute Maastricht, Maastricht University Medical Center, Universiteitssingel 50, 6229 ER Maastricht, The Netherlands; [7]Department of Clinical Pharmacology and Pharmacoepidemiology, University Hospital Heidelberg, Im Neuenheimer Feld 410, 69120 Heidelberg, Germany; [8]Department of Cardiac Surgery, University Hospital Heidelberg, Im Neuenheimer Feld 420, 69120 Heidelberg, Germany; [9]Department of Large Animal Internal Medicine, Equine Cardioteam, Faculty of Veterinary Medicine, Ghent University, Salisburylaan 133, B-9820 Merelbeke, Belgium; and [10]Digital Health Center, Berlin Institute of Health (BIH), Anna-Louisa-Karsch-Straße 2, 10178 Berlin, Germany[11]Health Data Science Unit, BioQuant, Faculty of Medicine, University of Heidelberg, Im Neuenheimer Feld 267, 69120 Heidelberg, Germany

Received 24 October 2020; editorial decision 12 May 2021; online publish-ahead-of-print 24 May 2021

See the editorial comment for this article 'Not the classical serendipity: does doxapram treat atrial fibrillation?', by Aiste Liutkute *et al.*, https://doi.org/10.1093/cvr/cvac044.

Aims TASK-1 ($K_{2P}3.1$) two-pore-domain potassium channels are atrial-specific and significantly up-regulated in atrial fibrillation (AF) patients, contributing to AF-related electrical remodelling. Inhibition of TASK-1 in cardiomyocytes of AF patients was shown to counteract AF-related action potential duration shortening. Doxapram was identified as a potent inhibitor of the TASK-1 channel. In this study, we investigated the antiarrhythmic efficacy of doxapram in a porcine model of AF.

Methods and results Doxapram successfully cardioverted pigs with artificially induced episodes of AF. We established a porcine model of persistent AF in domestic pigs via intermittent atrial burst stimulation using implanted pacemakers. All pigs underwent catheter-based electrophysiological investigations prior to and after 14 days of doxapram treatment. Pigs in the treatment group received intravenous administration of doxapram once per day. In doxapram-treated AF pigs, the AF burden was significantly reduced. After 14 days of treatment with doxapram, TASK-1 currents were still similar to values of sinus rhythm animals. Doxapram significantly suppressed AF episodes and normalized cellular electrophysiology by inhibition of the TASK-1 channel. Patch-clamp experiments on human atrial cardiomyocytes, isolated from patients with and without AF could reproduce the TASK-1 inhibitory effect of doxapram.

Conclusion Repurposing doxapram might yield a promising new antiarrhythmic drug to treat AF in patients.

*Corresponding author. Tel: +49 6221 568187; fax: +49 6221 565724, E-mail: Constanze.Schmidt@med.uni-heidelberg.de

Graphical Abstract

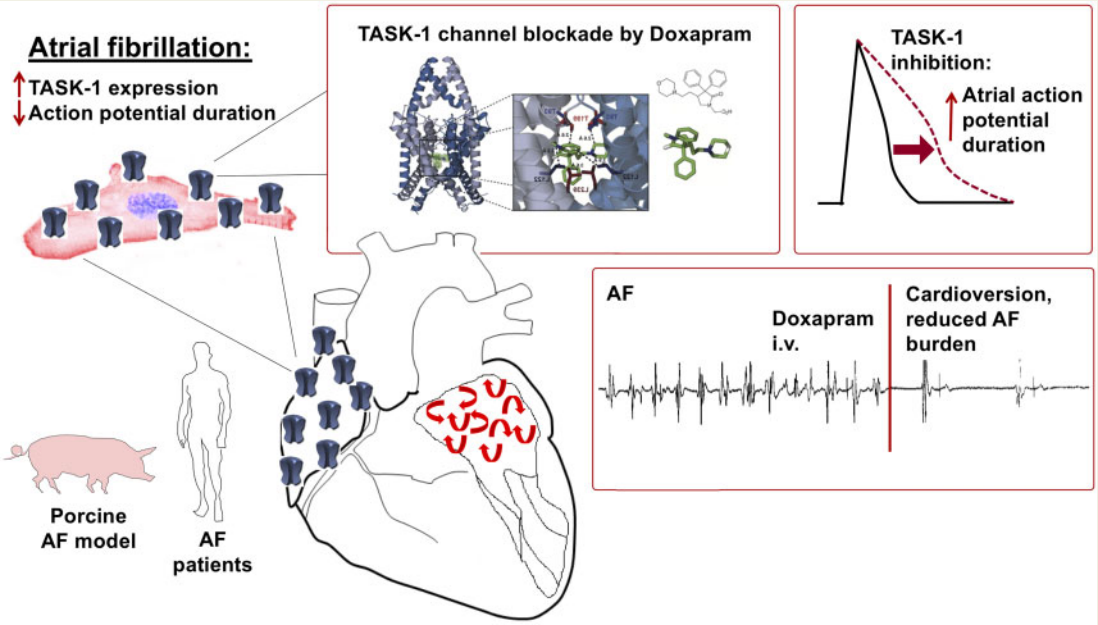

Keywords • Antiarrhythmic pharmacotherapy • Arrhythmia • Atrial fibrillation • Doxapram • Electrical remodelling • Potassium channel • Rhythm control • TASK-1 •

1. Introduction

Atrial fibrillation (AF) is by far the most common sustained cardiac arrhythmia.[1] Safe and effective pharmacological treatment of AF, however, still remains an unmet medical need. In the western world, ~3% of the population suffer from AF.[2] Its prevalence and incidence increase with age. Consecutively, it can be foreseen that the number of patients suffering from AF will increase in our ageing population.[3] The effectiveness of current pharmacological and interventional strategies against AF is still suboptimal resulting in an urgent need for novel therapeutic approaches.[4]

The tandem of P domains in a weak inward rectifying K^+ channel-related acid-sensitive K^+ channel (TASK-1; $K_{2P}3.1$) potassium channel is a member of the two-pore-domain potassium (K_{2P}-) channel family.[5,6] In the human heart, TASK-1 ($hK_{2P}3.1$) is specifically expressed in the atria. Recently, it was described that TASK-1 expression is up-regulated in patients suffering from AF, contributing to the pathological shortening of the atrial action potential duration (APD)[7,8] together with calcium handling abnormalities, increased repolarizing potassium currents, like I_{K1} as well as agonist-independent 'constitutive' $I_{K,\ ACh}$, and alterations in cell-to-cell electrical coupling.[9–13]

Therefore, TASK-1 channels represent a potential novel target for pharmacological rhythm control by counteracting AF-induced APD shortening. The TASK-1 current can be inhibited by experimental ion channel inhibitors as well as clinically used antiarrhythmic drugs.[14–17] For example, pharmacological inhibition of TASK-1 using the experimental inhibitor A293 was recently shown to exhibit atrial-specific antiarrhythmic properties in our porcine large animal model.[18,19]

The pyrrolidinone derivative doxapram, clinically employed as a respiratory stimulant for over half a century, was recently identified as a potent inhibitor of TASK-1 channels.[20–23] Doxapram acts on both brainstem respiratory centres and peripheral carotid chemoreceptors, where TASK-1 and TASK-3 channels are abundantly expressed.[24] Carotid body type 1 cells are regulated via oxygen-sensitive K^+ currents, which are most likely carried by TASK channels and doxapram probably acts by inhibiting these channels.[22,24] IC_{50} values of doxapram on TASK-1 are well within its therapeutic range, and thus this FDA- and EMA-approved drug might bear the potential to be used for rhythm control in AF patients.

Our preclinical trial aimed to assess the antiarrhythmic potential of pharmacological TASK-1 channel inhibition by doxapram using clinically relevant large animal models of acute episodes of paroxysmal AF and persistent AF. Here, the respiratory stimulant doxapram was successfully applied for cardioversion of paroxysmal AF episodes as well as rhythm control of persistent AF. Additionally, patch-clamp experiments on isolated human atrial cardiomyocytes from patients with AF could confirm an efficient antiarrhythmic effect of doxapram. Finally, the antiarrhythmic potential of TASK-1 inhibition by doxapram could be reproduced by multiscale *in silico* modelling of human atrial electrophysiology. Altogether, these studies provide a clear rationale for the doxapram conversion to sinus rhythm (SR) (DOCTOS) trial (EudraCT No: 2018-002979-17), which investigates whether doxapram can cardiovert AF in patients.

2. Methods

For a detailed description of the employed methodology, please refer to the Supplementary material online.

2.1 Animal handling

Animal experiments were carried out in accordance with the Guide for the Care and Use of Laboratory Animals as adopted and promulgated by the US National Institutes of Health (NIH publication No. 86-23, revised 1985), with EU Directive 2010/63/EU, and with the current version of the German Law on the Protection of Animals. Approval for experiments involving pigs or *Xenopus laevis* was granted by the local Animal Welfare Committee (Regierungspraesidium Karlsruhe, Germany, reference numbers A-38/11, G-221/12, G-296/14, G-217/18, and G-165/19). Following sedation with azaperone [5 mg/kg, intramuscular (*i.m.*); Elanco, Bad Homburg, Germany], midazolam (1 mg/kg, *i.m.*; Hameln Pharma Plus GmbH, Hameln, Germany), and ketamine (10 mg/kg, *i.m.*; Zoetis Deutschland GmbH, Berlin, Germany), pigs were anaesthetized with propofol [1.5 mg/kg bolus, intravenous (*i.v.*) followed by 4–8 mg/kg/h, *i.v.*; Fresenius Kabi, Bad Homburg, Germany]. After completion of echocardiography and electrophysiological (EP) studies anaesthesia was perpetuated with isoflurane (0.5–2 vol.%; Baxter Deutschland GmbH, Heidelberg, Germany). For analgesia buprenorphine (0.02 mg/kg, *i.v.*; Bayer Vital GmbH Tiergesundheit, Leverkusen, Germany) was administered. Porcine hearts were explanted at the end of final surgery after euthanization by *i.v.* injection of 40 mL potassium chloride (1 mol/L) in deep anaesthesia.

2.2 Porcine AF model

Induction of persistent AF in pigs was carried out by atrial burst pacing via an implanted cardiac pacemaker (St. Jude Medical, St. Paul, MN, USA). To prevent tachycardia-induced heart failure, atrioventricular (AV) node ablation was performed under fluoroscopic guidance. Acute AF was induced via right-atrial burst stimulation (400–1200 min^{-1}) during EP studies.

2.3 Patients

The study protocol involving human tissue samples was approved by the ethics committees of the Medical Faculty of Heidelberg University (Germany; S-017/2013). Written informed consent was obtained from all patients and the study was conducted in accordance with the Declaration of Helsinki. A total of 12 patients with SR or chronic AF (cAF) undergoing open heart surgery for coronary artery bypass grafting, heart valve repair or valve replacement were included in the study.

2.4 Patch-clamp electrophysiology

Human and porcine atrial myocytes were isolated freshly as described in the Supplementary material online. EP recordings were carried out at room temperature (22–23°C) using the whole-cell patch-clamp configuration.

2.5 Molecular biology and *xenopus* oocyte electrophysiology

For oocyte preparation, ovarian lobes of female *Xenopus laevis* frogs (Xenopus Express, Le Bourg, France) were surgically removed in aseptic techniques, anaesthetized with tricaine solution (1 g/L, pH 7.5, 15°C). After the final collection of oocytes, anaesthetized frogs were killed by decerebration and pithing. Copy RNA was synthesized, using the mMESSAGE mMACHINE T7 Transcription Kit (Thermo Fisher Scientific, Waltham, MA, USA) and injected into stages V and VI defolliculated *Xenopus laevis* oocytes as described earlier.[7]

3. Results

3.1 Doxapram inhibits human and porcine TASK-1 channels

Major anatomical and physiological analogies to humans constitute specific advantages of using pigs as a large animal model in cardiovascular research. Human (h) and porcine (p) TASK-1 channels display a large degree of homology, resulting in comparable functional and regulatory properties.[18,25] *In silico* docking simulations of doxapram into the intracellular pore of an open-state pTASK-1 homology model based on the recently revealed crystal structure of hTASK-1 (PDB ID: 6RV2)[26] predicted that its binding site is located in close proximity to the pore-lining amino acids T93, L122, T199, and L239 (*Figure 1A–C*). It was experimentally shown that these amino acid residues contribute to the drug-binding site of the high affinity TASK channel blocker A293[27] and likewise mediate doxapram binding.[21,23] A comparison of the structure and predicted drug-binding site within the TASK-1 inner channel pore is presented in Supplementary material online, *Figure S1*.

Following heterologous expression in *Xenopus oocytes*, human and porcine TASK-1 channel subunits give rise to comparable macroscopic currents (*Figure 1D and G*). Outward potassium currents were measured using the two electrode voltage-clamp technique 24–72 h after injection of copy RNA encoding either human or porcine TASK-1 orthologs. Currents were elicited by application of depolarizing test pulses (500 ms), applied in 20-mV increments from a holding potential of -80 mV to +60 mV (0.2 Hz, see *Figure 1D and G*). Current amplitudes were measured at the end of the +20 mV pulse. After a control period with no significant amplitude changes (10 min), administration of doxapram (10 µmol/L, 30 min) resulted in rapid decline of outward potassium currents (human: 71.8±3.6%, $n = 7$, $P = 0.0002$; porcine: 73.4±8.0%, $n = 4$, $P = 0.003$; *Figure 1D–I*). Doxapram blockade did not affect the current–voltage relationship of human or porcine TASK-1 orthologs. Inhibition of TASK-1 currents by doxapram was concentration-dependent (*Figure 1F and I*). Half-maximal concentrations (IC_{50}) of human and porcine TASK-1 by doxapram were 0.88 µmol/L [1σ-confidence interval (CI), (0.46 µmol/L, 1.07 µmol/L)] and 0.93 µmol/L [1σ-CI, (0.43 µmol/L, 1.31 µmol/L)] (n = 3–24 cells per concentration step).

Among human atrial potassium channels, doxapram (5 µmol/L) displayed specific TASK channel inhibition without significantly affecting heterologously expressed TASK-4, TREK-2, $K_{ir}2.1$, $K_{ir}3.1/K_{ir}3.4$, $K_V1.4$, $K_V1.5$, $K_V2.1$, $K_V4.3$, MaxiK, $Na_V1.5$, or $Ca_V1.2$ channels (*Figure 1J and K*). TASK-3 channels were blocked by doxapram with similar efficiency as TASK-1. However, our former studies pointed towards negligible cardiac expression levels of TASK-3.[7,28] Application of 100 µmol/L doxapram was associated with mild to moderate off-target effects on $K_V1.4$, $K_V2.1$, and hERG currents (Supplementary material online, *Figure S2*).

3.2 *In vivo* antiarrhythmic properties of doxapram in a porcine large animal model

Upon acute intravenous (*i.v.*) administration of doxapram [2 mg/kg body weight (BW)] in healthy control pigs (n = 3 German landrace pigs of both sexes), a rapid peak and decline of doxapram plasma levels could be observed (*Figure 2A*). Surface electrocardiograms (ECGs), recorded 5 min after *i.v.* administration of doxapram (2 mg/kg BW), did not show relevant alterations in PQ, QRS, QT, or QTc intervals compared to baseline conditions (n = 7 independent experiments performed on N = 4

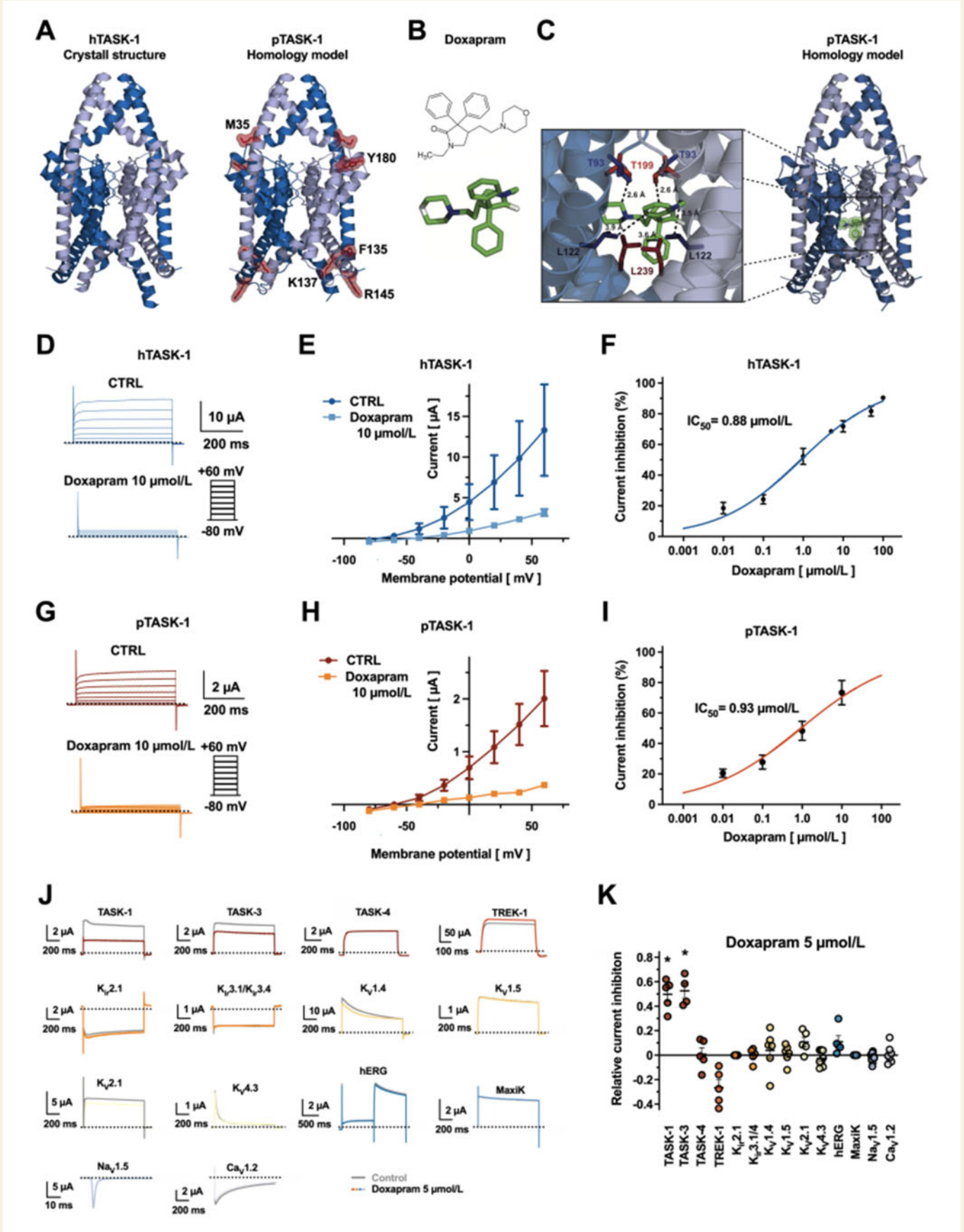

Figure 1 Pharmacological effects of doxapram on TASK-1 potassium channels. (*A*) *Left:* hTASK-1 crystal structure.[26] *Right:* homology model of pTASK-1 based on the respective crystal structure. Differences in hTASK-1 and pTASK-1 amino acid sequence are indicated in red. (*B*) Chemical structure of

individual pigs (*Figure 2B*). A trend towards increased heart rates was observed after application of doxapram (1 mg/kg BW: 15.9% increase; 2 mg/kg BW 20.2% increase) (*Figure 2C*). Invasive blood pressure recordings performed in anaesthetized pigs revealed a slight trend towards increased systolic, diastolic, and mean blood pressure levels under doxapram treatment that did not reach statistical significance (*n*/*N* = 7/4) (*Figure 2D*). Atrial effective refractory periods (AERPs) measured at different basic cycle lengths (BCL), were significantly prolonged upon TASK-1 inhibition by doxapram consistent with class-III antiarrhythmic effects (*Figure 2E*). The AERP measured at a BCL of 500 ms ($AERP_{500}$) increased from 216.4±24.4 ms under control conditions to 251.4±22.1 ms after administration of 1 mg/kg BW doxapram, and further increased to 254.7±19.7 ms after 2 mg/kg BW doxapram ($P = 0.0011$ and $P = 0.0036$; *n*/*N* = 6/4) (*Figure 2E*). The $AERP_{400}$ was prolonged from 212.1±19.8 ms to 232.9±18.4 ms after *i.v.* injection of 1 mg/kg BW doxapram, and to 237.9±20.9 ms after *i.v.* injection of 2 mg/kg BW doxapram ($P = 0.029$ and $P = 0.00026$; *n*/*N* = 6/4) (*Figure 2E*); the $AERP_{300}$ was prolonged from 170.0±15.7 ms to 205.0±13.5 ms at 1 mg/kg BW doxapram, and to 212.5±23.5 ms at 2 mg/kg BW doxapram ($P = 0.0094$ and $P = 0.046$, respectively; *n*/*N* = 6/4) (*Figure 2E*).

3.3 Pharmacological cardioversion of acute paroxysmal AF episodes by *i.v.* doxapram treatment

Subsequently, the antiarrhythmic potential of doxapram-induced prolongation of AERP was studied in a porcine model of acute episodes of paroxysmal AF. AF episodes were artificially induced by right-atrial burst pacing (10 V, 150–50 ms cycle length, 2–8 s duration) during EP studies. Following a control period of 5 min to confirm stability of the induced AF episode, pigs were treated with different concentrations of doxapram (*Figure 2F*). Whereas doxapram doses of 1 mg/kg BW (empty circles) did not result in cardioversion of AF during an observation period of 10 min, strikingly, doxapram doses ≥1.5 mg/kg BW (blue dots) resulted in a 100% cardioversion rate. After *i.v.* administration of doxapram, the time to cardioversion was monitored in surface and intracardiac ECGs. The average time to cardioversion was 2.5±0.6 min after *i.v.* administration of doxapram (*n* = 17) (*Figure 2G*). On average, doses of 1.85 mg/kg BW were sufficient for cardioversion (*n* = 17) (*Figure 2H*).

3.4 Effects of continuous doxapram treatment in a porcine model of persistent AF

To study the efficacy of pharmacological TASK-1 inhibition by doxapram in rhythm control, doxapram was administered daily in a porcine model of persistent AF. In all animals, echocardiography and invasive EP studies were conducted (Supplementary material online, *Figure S3*), a dual chamber pacemaker was implanted, and an AV node ablation was performed in animals randomized to AF groups to prevent tachycardiomyopathy as a consequence of AF induction.[19,29] Ventricular backup pacing was provided via the implanted pacemakers. Subsequently, 24 pigs were randomized to an AF group (*n* = 12) or a SR control group (*n* = 12) with deactivated pacemakers (*Figure 3A*). In the AF group, AF was induced by right-atrial burst stimulation. Both study cohorts were divided into a treatment arm (*n* = 5–6) with daily doxapram administration (2 mg/kg BW *i.v.*) and a control arm with sham treatment (0.9% NaCl solution; *n* = 5–6). During the 14 days follow-up period, atrial burst stimulation was alternated with pacing-free intervals for automatic rhythm assessment by the pacemakers. A programmable biofeedback algorithm was implemented in the pacing devices that interrupted burst pacing when endogenous AF was detected. At the end of the observation period, AF pigs underwent electrical cardioversion. Echocardiography and EP studies were repeated, and isolated right-atrial cardiomyocytes of all study pigs were subjected to patch-clamp measurements (*Figure 3A*). Additional hemodynamic and echocardiographic characteristics of the study pigs, obtained on Day 0 and Day 14 are given in Supplementary material online, *Table S1*. Representative surface ECGs, recorded on Day 14 are depicted in *Figure 3B* and P waves are highlighted with black dots. Again, doxapram treatment did not result in significant surface ECG changes. TASK-1 inhibition by chronic doxapram treatment did not significantly affect the function of the sinus node (*Figure 3C*). Further analyses of ECG parameters and representative intracardiac recordings of the rhythm state by the implanted devices are shown in Supplementary material online, *Figures S4 and S5*. No significant changes of the sinus node recovery times (SNRTs) measured after 30 s of overdrive suppression and the corrected sinus node recovery times (cSNRT) were observed. Furthermore, sinoatrial conduction times (SACT), measured by applying the Narula[30] or Strauss[31] method, remained unchanged (*Figure 3C*).

Figure 1 Continued

monohydrated pyrrolidinone derivative doxapram. (*C*) Simulation of doxapram docking to the inner channel pore of pTASK-1. Excerpts illustrate the interactions of doxapram with pore-associated amino acids. (*D–I*) Human and porcine TASK-1 ion channel subunits, heterologously expressed in *Xenopus laevis* oocytes, are inhibited by doxapram (10 µmol/L) to a similar extent. (*D* and *G*) Representative current traces of hTASK-1 (*D*) and pTASK-1 (*G*) before (CTRL) and after 10 µmol/L doxapram (*n* = 3–4). (*E* and *H*) Current–voltage relationships of human (*E*) and porcine (*H*) TASK-1 before (CTRL) and after doxapram (*n* = 3–4). (*F* and *I*) Concentration–response relationships for the effect of doxapram, on human (*F*) and porcine (*I*) TASK-1 (*n* = 3–24). (*J* and *K*) TASK-specificity of doxapram among atrial potassium channels assessed in oocytes (*n* = 4–15 individual cells). Significant current reduction was observed in TASK-1 and non-cardiac TASK-3 subunits. (*J*) Representative current traces recorded under control conditions (grey) and after doxapram (5 µmol/L, 30 min) by application of voltage pulses from -80 to +40 mV for TASK-1, TASK-3, TASK-4, TREK-1, MaxiK, $K_V1.4$, $K_V1.5$, $K_V2.1$, and $K_V4.3$, pulses from -160 to 0 mV for $K_{ir}2.1$ and $K_{ir}3.1/K_{ir}3.4$ or a double step from -80 to +20 mV and -40 mV for hERG. For $Na_V1.5$ currents, the voltage was stepped from a holding potential of -80 to -30 mV, utilizing a digital leak subtraction with a *p* over *n* protocol of *n* =4. For $Ca_V1.2$ voltage was stepped from -80 to +10 mV for 1 s, sweep time interval was 30 s. (*K*) Relative current inhibition levels are compared (*n* = 4–15 individual cells). Data for $Ca_V1.2$ recordings were corrected for rundown. Dashed lines: zero current level. Data are presented as mean±SEM. *, $P < 0.05$ vs. respective CTRL for Student's *t*-tests.

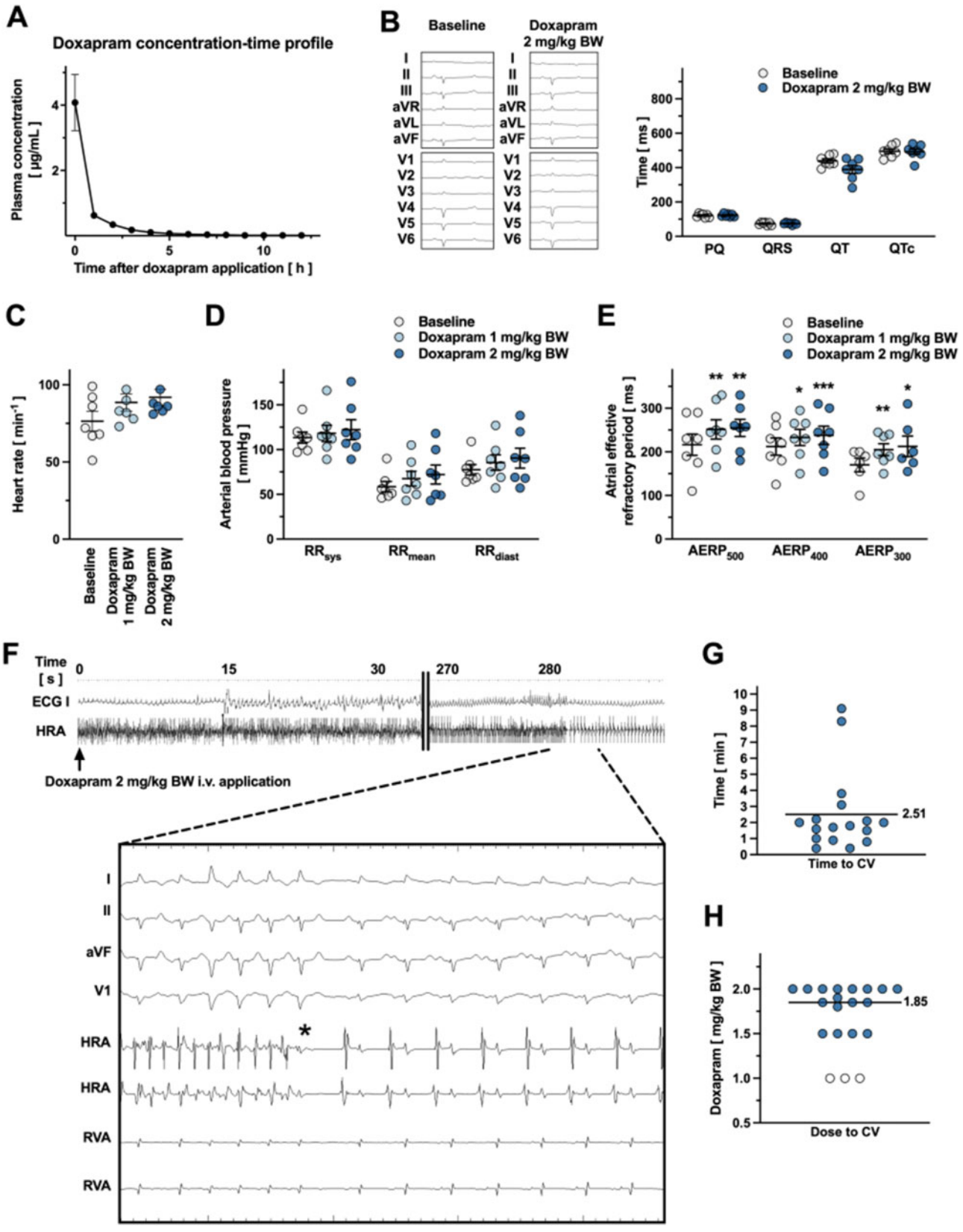

Figure 2 Acute effects of doxapram on atrial electrophysiology, insights from a porcine large animal model. (*A*) Doxapram plasma concentrations measured in 60 min intervals after intravenous administration of doxapram, 2 mg/kg BW (n = 3). (*B*) Representative surface ECGs recorded in pigs before and 10 min after doxapram administration, 2 mg/kg BW (n = 7 experiments performed on N = 4 pigs). (*C*) Upon administration of doxapram a non-significant trend towards faster heart rates could be observed (n/N = 7/4). (*D*) Systolic (RR_{sys}), diastolic (RR_{diast}), and mean (RR_{mean}) arterial blood pressure levels were not significantly changed by doxapram treatment (n/N = 7/4). (*E*) Administration of doxapram significantly prolonged the AERPs (n/N = 7/4). (*F–H*)

A mild trend towards an increased AV node conduction was observed in case of continuous treatment with doxapram (*Figure 3D*). The Wenckebach point, the time of AV nodal 2:1 conduction, and AV nodal effective refractory periods (AVNRP), measured at BCLs of 500 and 400 ms, were slightly shortened under doxapram treatment (*Figure 3D*). Notably, animals in the AF group received AV node ablations. Therefore, no measurements of AV nodal conduction could be performed in this group.

As expected, AERPs were significantly shortened in untreated AF pigs compared to SR pigs (*Figure 3E*). This observation is consistent with the atrial electrical remodelling, that is also observed in AF patients. Daily doxapram administration increased AERPs to levels observed in the SR control group, reflecting class-III antiarrhythmic effects (*Figure 3E*). No significant changes in VERPs were observed under continuous doxapram treatment again indicating absence of off-target effects at the level of ventricular electrophysiology (*Figure 3F*). After 14 days, animals in the AF group without treatment presented AF in 95% of the analysed surface ECG recordings (*Figure 3G*). In contrast, AF animals receiving daily doxapram *i.v.* treatment displayed AF in only 1% of the recorded ECGs (N = 5 animals; $P < 0.0001$). Thus, long-term doxapram treatment successfully prevented tachypacing-induced atrial remodelling. Measurements of doxapram plasma levels in blood samples of AF and SR animals taken before daily doxapram treatments indicate an initial saturation phase followed by a plateau phase that is reached 5–7 d after start of the continuous treatment (*Figure 3H*).

3.5 Effects of chronic doxapram treatment on cellular electrophysiology of atrial cardiomyocytes

Consecutively, effects of pharmacological TASK-1 inhibition by doxapram on atrial cellular electrophysiology were studied in isolated atrial cardiomyocytes from AF and SR pigs. Patch-clamp experiments were performed in the whole-cell configuration. A microscope image of an isolated porcine atrial cardiomyocyte is presented in *Figure 4A*. Representative isolated TASK-1 currents (i.e. differences in currents, recorded under control conditions and after application of 200 nmol/L A293) of the different experimental groups are shown in *Figure 4B and C*. A293-sensitive K^+ current densities were activated at potentials >-20 mV and showed Goldman–Hodgkin–Katz rectification, which is typical for K_{2P} channels (*Figure 4D–F*).[7,32] AF-associated up-regulation of TASK-1 resulted in a 8.6-fold up-regulation of TASK-1 current densities in comparison to SR controls ($P = 0.024$; n/N = 18–24/4–6; n, number of cells; N, number of pigs) (*Figure 4G*). Daily *i.v.* doxapram treatment of AF pigs attenuated TASK-1 current up-regulation by 85.2% ($P = 0.15$; n/N = 24–26/4–6) whereas no relevant changes in TASK-1 currents were observed between the SR control animals and SR animals under doxapram treatment ($P = 0.9$; n/N = 14–18/4–6 animals). Resting membrane potentials did not differ significantly among the four groups (Supplementary material online, *Figure S6*).

Atrial cardiomyocyte action potentials (APs) were studied under current-clamp conditions in isolated cells from all four study cohorts. Representative recordings are shown in *Figure 4H and I*. In untreated AF animals, APDs at 50% repolarization (APD_{50}) were 97.2±10.9 ms (n/N = 6/4) compared to 158.3±14.3 ms in the SR control group (n/N = 6/4; P = 0.0075) (*Figure 4J*). Under daily doxapram treatment, AF animals displayed APD_{50} values comparable to SR controls (157.2±4.7 ms; n/N = 17/4) (*Figure 4J*). Finally, TASK-1 inhibition in SR animals did not cause significant modulation of APD_{50} values (171.4±10.4 ms; $P = 0.38$ vs. SR control; n/N = 11/3) (*Figure 4J*). Similar results were obtained for APD_{90} measurements (*Figure 4K*). *KCNK3* qPCR expression analysis among atrial cardiomyocytes, non-myocytes, and cultured atrial fibroblasts points towards cardiomyocyte specific expression of TASK-1 (Supplementary material online, *Figure S7*).

3.6 Computational modelling of the doxapram effects on atrial electrophysiology in a single-cell and a tissue model

Computational modelling at single-cell and 2-dimensional tissue levels was employed to directly probe the EP and antiarrhythmic effects of doxapram-mediated TASK-1 inhibition. Our recent human atrial cardiomyocyte model with TASK-1 formulation was fitted to the experimentally obtained current–voltage relationship of human and porcine TASK-1 (*Figure 5A*, left and middle panels), and the concentration-dependent effect of doxapram on TASK-1 was incorporated (*Figure 5A*, right panels). The appropriate concentration of doxapram to simulate long-term (14 days) treatment was determined based on the TASK-1 measurements from the four experimental groups shown in *Figure 5*. A simulated concentration of 1 µmol/L doxapram reproduced the experimentally observed reduction in TASK-1 (*Figure 5B*). APD prolongation in the human atrial cardiomyocyte model with AF-related remodelling in response to acute application of 1 µmol/L doxapram was smaller than observed with long-term treatment in pigs. However, when combining the acute inhibition of TASK-1 with a reduction in AF-related remodelling, consistent with the experimentally observed antiarrhythmic effects of doxapram, the EP phenotype of long-term doxapram treatment could be closely reproduced (*Figure 5C*). Finally, the antiarrhythmic effect of such long-term doxapram treatment was investigated in homogeneous 2-dimensional tissue simulations. Re-entry was induced using an S_1S_2 pacing protocol with different coupling intervals in virtual tissue with and without AF-related remodelling in the absence or presence of the EP effects of long-term doxapram treatment (*Figure 5D*, left panels). The resulting vulnerable windows with the duration of re-entry induced for each S_1S_2 interval summarize the inducibility and stability of re-entry and the sum of re-entry durations over all S_1S_2 intervals provides an indication of total arrhythmogenic vulnerability. As expected, the arrhythmogenic vulnerability was considerably larger in the presence of AF-related remodelling (*Figure 5D*, right). Importantly, simulated long-term doxapram treatment reduced re-entry duration to values, observe in control

Figure 2 Continued

After induction of AF atrial rhythm was monitored for 5 min. When AF persisted different doses of doxapram were intravenously administered and time to cardioversion was measured. (*F*) Surface and intracardiac ECG recordings. The magnification visualizes time of cardioversion to SR marked with an asterisk. (*G*) Time to cardioversion of AF after infusion of doxapram (n/N = 17/17). (*H*) Doxapram dosages that were not effective (white circles) or effective for cardioversion (blue dots; n/N = 20/17). Data are shown as mean±SEM. *, $P < 0.05$; **, $P < 0.01$; ***, $P < 0.001$ vs. baseline for Student's *t*-tests. Where no asterisks are presented, no statistically significant difference was observed in Student's *t*-tests.

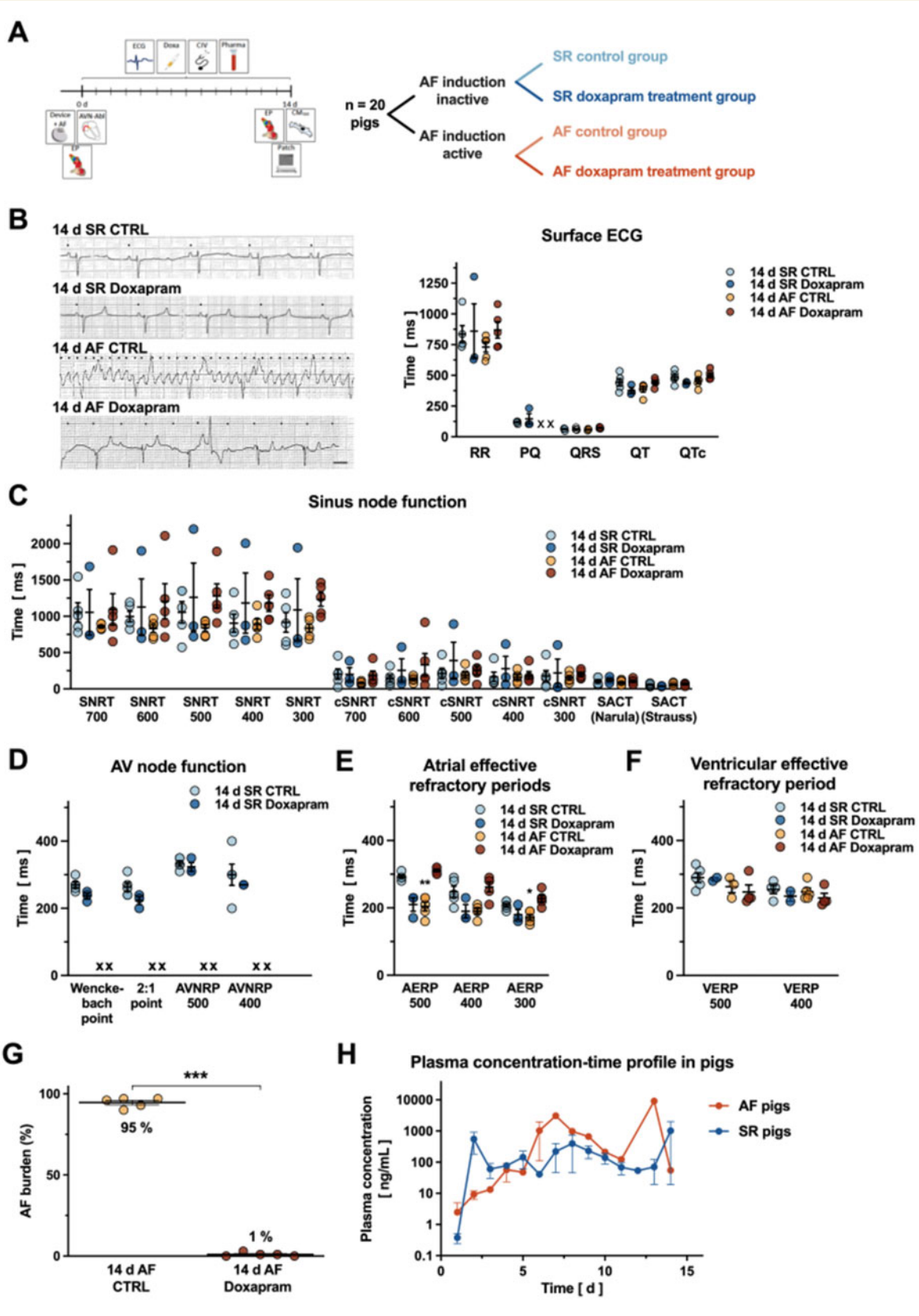

Figure 3 Safe and effective treatment of persistent AF using doxapram in a porcine disease model. (*A*) Experimental protocol: subsequent to an EP investigation and pacemaker implantation, 20 pigs were randomized to AF induction or a SR control (CTRL) group. AF and SR groups were divided into subgroups receiving intravenous doxapram or sham treatment. (*B*) Surface ECGs from all 4 subgroups on day 14 (*left panel*). Black dots indicate *P* waves. Scale bar (bottom right) denotes 200 ms. *Right*: mean surface ECG parameters. PQ intervals could not be measured after AV node ablation in the AF groups ($n = 4–5$). (*C*) SNRT, cSNRT, and SACT ($n = 4–5$). (*D*) AVNRP measured in SR animals ($n = 4–5$). (*E*) AERPs were significantly reduced in the AF-induction group and

animals. Similar results were obtained in the presence of 100 µmol/L doxapram, assuming selective TASK-1 inhibition (Supplementary material online, *Figure S8A and B*). When simulating potential off-target effects at this high concentration (36.7% inhibition of rapid delayed-rectifier K^+ current; 28.0% inhibition of transient-outward K^+ current and 17.3% inhibition of ultra-rapid delayed-rectifier K^+ current; based on Supplementary material online, *Figure S2*), doxapram-induced repolarization prolongation was increased, resulting in a minor augmentation of antiarrhythmic effects in tissue simulations (Supplementary material online,

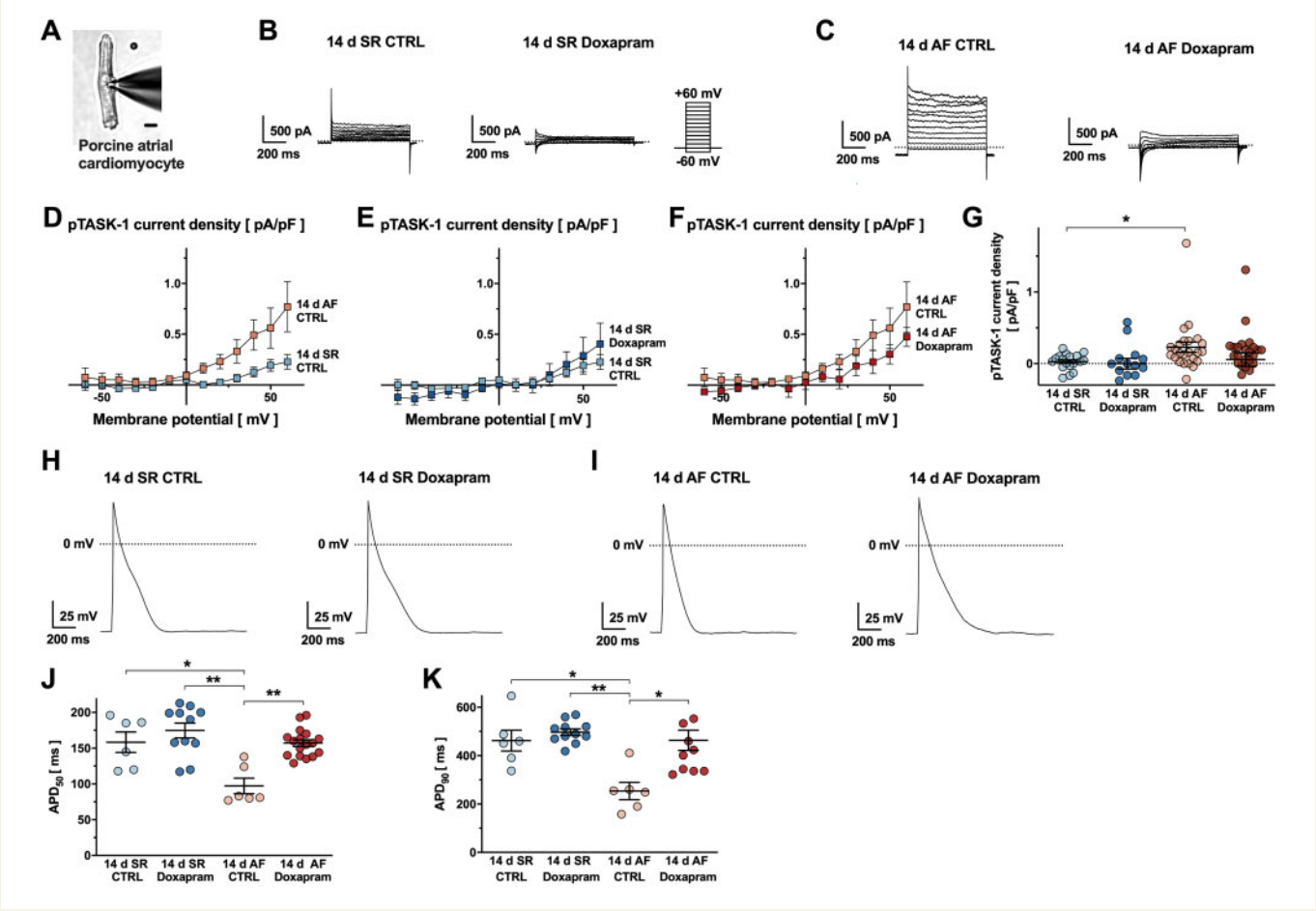

Figure 4 Patch-clamp recordings of atrial TASK-1 currents and APs of SR and AF pigs during long-term doxapram treatment. (*A*) Isolated porcine atrial cardiomyocyte attached to a patch-clamp micropipette (scale bar: 25 µm). (*B* and *C*) TASK-1 current densities recorded from atrial cardiomyocytes from AF or SR pigs after 14 days. The pulse protocol used in voltage–clamp measurements is depicted in panel (*B*). (*D–F*) Dependence of mean step current densities on test potentials for the treatment and control groups (n = 11–26 cells, from N = 4–6 different animals per group). (G) Comparison of average A293-sensitive current densities, quantified at the end of +20 mV pulse. (*H–I*) Representative AP recordings of atrial cardiomyocytes. (*H–I*) Comparison of corresponding average AP durations at 50% repolarization (APD_{50}; *J*) or 90% repolarization (APD_{90}; *K*) of experimental groups (n = 6–17 cells, isolated from N = 3–4 animals per group). Data are shown as mean±SEM. Dashed lines indicate zero current and potential levels. *, $P < 0.05$;**, $P < 0.01$ from Student's *t*-tests.

Figure 3 Continued

could be restored by doxapram treatment (n = 4–5). *, $P < 0.05$; **, $P < 0.01$ vs. 14 days SR CTRL in Student's *t*-tests. (*F*) No statistically significant differences of ventricular ERPs were observed (n = 4–5). (*G*) AF burden (i.e. diagnosis of AF in daily surface ECGs in relation to the cumulative number of surface ECGs, documented during the 14 days follow-up period) was significantly reduced by doxapram treatment (n = 5). ***, $P < 0.001$ vs. 14 days AF CTRL in Student's *t*-tests. (*H*) Plasma levels of doxapram in AF and SR animals in daily blood samples (n = 5). Where no asterisks are presented, no statistically significant difference was observed in Student's *t*-tests.

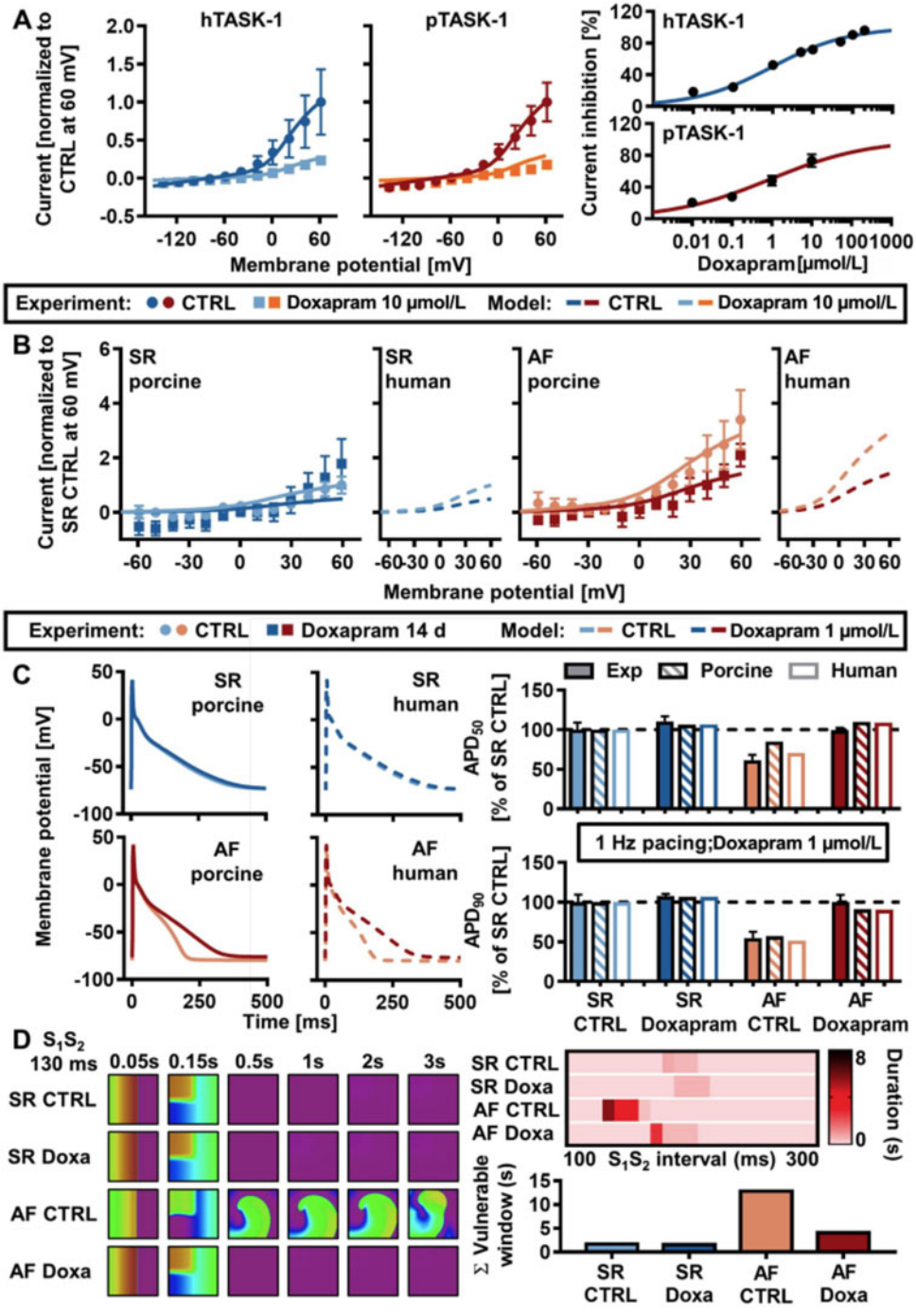

Figure 5 *In silico* analysis of the effects of doxapram on human atrial electrophysiology and arrhythmogenesis. (*A*) Voltage dependence of human and porcine TASK-1 in the absence (dark symbols/lines) or presence (light symbols/lines) of 10 µmol/L doxapram (left and middle), concentration–dependent inhibition of TASK-1 by doxapram (right) in experiments (symbols; data from *Figure 1*) and model (lines). (*B*) Voltage dependence of TASK-1 currents in SR and AF pigs with sham treatment (CTRL) or treated with doxapram (symbols; data from *Figure 4*) and in the human atrial cardiomyocyte model with pTASK-1 (solid lines) or hTASK-1 (dashed lines). (*C*) Validation of AP properties of the computer model with human or porcine TASK-1 without (SR) or with AF-related remodelling in the absence (CTRL) or presence of the EP effects of long-term (14 days) doxapram treatment (simulated as TASK-1 inhibition by 1 µmol/L doxapram and 75% reduction in AF-related electrical remodelling). Bar charts show relative changes in AP duration at 50% and 90% of repolarization (APD_{50} and APD_{90}) in models compared to experimental data from *Figure 4*. (*D*) Snapshots of simulated re-entry initiated by an S_1S_2 interval of 130 ms in 2-dimensional human atrial tissue models with or without AF-related remodelling in the absence (CTRL) or presence of the EP effects of long-term doxapram treatment (Doxa; left), and the vulnerable windows with re-entry duration for different S_1S_2 interval together with the sum of all re-entry durations, representing total arrhythmogenic risk.

Figure S8C and D). Together, these data support the pronounced antiarrhythmic effect of long-term doxapram treatment.

3.7 Effects of doxapram on human atrial cardiomyocytes isolated from SR and cAF patients

Finally, our findings regarding rhythm control in pigs with induced AF were evaluated in tissue samples from AF patients. To this end, atrial cardiomyocytes isolated from patients with cAF or SR were exposed to doxapram. Tissue samples were taken from patients undergoing open heart surgery for valve repair, replacement or coronary artery bypass grafting (Supplementary material online, *Table S2*). A microscope image of an isolated human atrial cardiomyocyte is shown in *Figure 6A*. Representative doxapram-sensitive background potassium currents from voltage-clamp recordings using the patch-clamp technique in whole-cell configuration are shown in *Figure 6B*. Similar to porcine atrial cardiomyocytes, Goldman–Hodgkin–Katz rectification was observed (*Figure 6C*). Doxapram-sensitive potassium background currents recorded from cAF cells were 2.9-fold higher than in SR controls (P = 0.02; n/N = 6–15/4–8) (*Figure 6D*).

Collectively, these results point towards class-III antiarrhythmic effects of doxapram in native human atrial cardiomyocytes, which were even enhanced in cells isolated from AF patients.

4. Discussion

4.1 Antiarrhythmic potential of doxapram

In the development of novel antiarrhythmic drugs, atrial selectivity is essential to prevent potential life-threatening side effects on ventricular electrophysiology.[4] In the human heart, TASK-1 channels are predominantly expressed in the atria.[7] Such atrial specificity was also observed in domestic pigs,[19,29] but not in small animals (e.g. mice).[28] Upon heterologous expression of TASK-1 in *Xenopus laevis* oocytes, doxapram has a similar affinity for human and porcine orthologs with IC_{50} values of 0.88 and 0.93 µM, respectively. Similar results were obtained in patch-clamp experiments performed on mammalian cells, with IC_{50} values of TASK-1 for doxapram inhibition in the single-digit micromolar range.[23]

Taking the substantial costs and the long timespan associated with drug development into account, repurposing of clinically established drugs with known tolerability becomes an attractive option.[33] Utilization of the FDA- and EMA-approved drug doxapram may therefore accelerate the evaluation of TASK-1 as a promising target for AF therapy in first clinical trials.

Our present data provide a proof-of-concept that blockade of atrial TASK-1 currents by doxapram exerts class-III antiarrhythmic effects *in vivo* sufficient for cardioversion as well as rhythm control of AF, induced in pigs. Pharmacological inhibition of atrial TASK-1 currents using

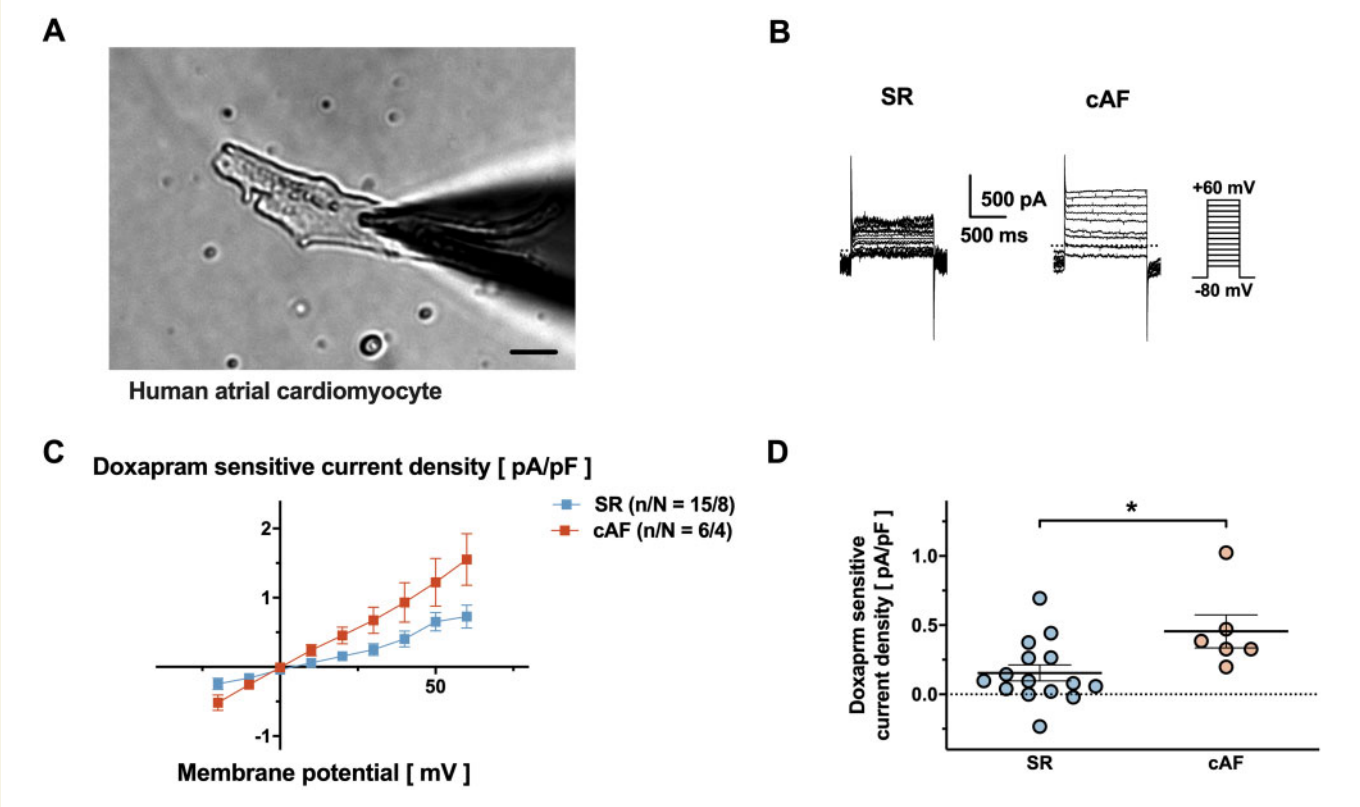

Figure 6 Effects of doxapram on human atrial cardiomyocytes from SR controls and AF patients. (*A*) Isolated human atrial cardiomyocyte (scale bar: 25 µm). (B–C) Potassium currents in human atrial cardiomyocytes after 100 µmol/L doxapram. (*B*) Representative current recordings for cardiomyocytes from SR and cAF patients. (*C*) Dependence of mean step current densities on the respective test pulse potentials (n = 6–15 cells, from 4–8 patients per group; no statistical significance in Bonferroni corrected Mann–Whitney tests). (*D*) Comparison of mean doxapram-sensitive current densities at +20 mV. Data are shown as mean±SEM. Zero current levels are indicated by dashed lines. *, $P < 0.05$ from Mann–Whitney test.

the respiratory stimulant drug doxapram facilitated pharmacological cardioversion of induced AF episodes through prolongation of atrial refractoriness. Furthermore, long-term doxapram treatment resulted in rhythm control in a clinically relevant large animal model of persistent AF. No relevant side effects were observed on the basis of ventricular EP parameters. At a cellular level, doxapram treatment prevented up-regulation of TASK-1 currents and APD shortening in isolated porcine atrial cardiomyocytes. The effects of TASK-1 current inhibition and APD prolongation could be reproduced and mechanistically explained using a computational model of an atrial cardiomyocyte. Multicellular model simulations further replicated the effects on AERPs, confirmed the resulting antiarrhythmic efficacy of doxapram and extrapolated our findings to a broad range of experimental conditions.

Additionally, our study confirms the role of TASK-1 current up-regulation in AF-related electrical remodelling, and its implication in shortening of the atrial APD and AERP. Our observations are in line with previous findings in human atrial cardiomyocytes, isolated from AF patients.[7,8] Enhanced atrial repolarizing K^+ currents and shortening of refractoriness represent classical characteristics of AF-associated electrical remodelling, promoting re-entry and perpetuation of the arrhythmia.[9,12] In this context, TASK-1 inhibition might serve as a mechanism-based antiarrhythmic concept.

While TASK-1 channels display atrial-specific expression patterns within the human heart, TASK-1 and closely related TASK-3 channels are expressed in several other organ systems where they control numerous important physiological processes. TASK-1 expression was reported in the brain, lung, liver, kidney, adrenal gland, pancreas, placenta, ovary, prostate, small intestine, and chondrocytes.[34–36] Animal models pointed towards a role of TASK-1 currents in mediating anaesthetic regulation of neuronal activity, breathing stimulation, regulation of thermogenesis, pulmonary vascular tone, immunoresponse, aldosterone secretion, and tumorigenicity.[20,36–39] Thus, when employing inhibitors of TASK-1 channels for treatment of AF, care has to be taken not to interfere with other organ functions. Following an initial saturation phase, doxapram plasma levels of our study pigs reached a plateau phase in the range of 0.1–1 μg/mL. When applied as a respiratory stimulant, therapeutic plasma levels of doxapram were reported to reach 2 μg/mL.[24]

In dogs, an acute increase in systemic blood pressure (10–20 mmHg) was reported after doxapram treatment, accompanied by an increase (∼25%) in cardiac output.[24,40] A clinical study in patients, receiving doxapram following thoracic surgery found no change in blood pressure or hemodynamics.[41] The observation that doxapram, applied during right heart catheterization of patients suffering from chronic bronchitis, results in a ∼10 mmHg increase in pulmonary artery pressure[42] could be attributed to TASK-1 channel expression in pulmonary artery smooth muscle cells.[43] Another potential side effect described in the use of doxapram in neonatology is an increased incidence of hypokalaemia, which is associated with increased aldosterone levels and is reversible after discontinuation.[44,45] This side effect could also be explained by TASK channel inhibition, as the knockout of TASK channel genes in mice was shown to result in a phenotype of primary hyperaldosteronism.[37]

Doxapram has been routinely employed as a respiratory stimulant in human and veterinary medicine for over half a century.[24,46] However, to our best knowledge, this study is the first systematic characterization of its antiarrhythmic properties, because previous studies only reported effects of doxapram on the QT interval[47] or on surface ECG parameters.[48–50] Early studies in anaesthetized dogs and patients with structural heart diseases showed an increase of ventricular ectopy after doxapram treatment.[48,50] It remains, however, uncertain whether this ectopy was primarily caused by EP effects of doxapram or by an increased sympathoadrenergic drive, increased cardiac output or an increased respiratory drive. Interestingly, De Villiers et al.[49] reported the development of a second-degree AV block in three cases of premature infants treated with high doses of doxapram (1.47 mg/kg/h or 15–18.5 mg/kg four times per day) that could be related to adverse effects on cardiac conduction. Furthermore, occurrence of junctional rhythms was described in dogs treated with high doxapram doses (5 mg/kg).[48] In comparison to the studies by De Villiers *et al.*[49] and Maillard *et al.*,[47] however, our experiments showed no significant effects of doxapram on ventricular repolarization.

Current pharmacological therapies for rhythm control in AF patients as well as cardioversion are still limited. Due to its atrial-specific expression, up-regulation in AF, and its functional connection to the APD length, TASK-1 might be a promising target for AF suppression. In this study, we observed that doxapram, a specific TASK-1 inhibitor, could be successfully administered for cardioversion and rhythm control of AF in pigs. Our experiments in porcine atrial cardiomyocytes showed an up-regulation of TASK-1 in AF, resulting in elevated TASK-1 currents that could be inhibited by doxapram treatment, resulting in values, observed among SR cardiomyocytes. Due to the indication of doxapram as a breathing stimulant, its antiarrhythmic effect might be studied in sleep apnoea patients that frequently suffer from AF. Based on the preclinical results in this animal study, we started the DOCTOS trial (EudraCT No: 2018-002979-17) in 2019 as the first clinical trial evaluating the efficacy of doxapram for AF cardioversion.

4.2 Potential limitations

The porcine animal model of right-atrial tachypacing-induced AF might differ from clinically observed spontaneous AF, regarding the pathophysiological mechanism of arrhythmogenesis. Previous EP studies, however, showed similar functional and molecular characteristics of the porcine AF model and AF in human.[18,25] Further, AF induction and antiarrhythmic drug therapy were started in parallel therefore, the model may reflect the clinical situation of a patient with a mild atrial substrate at the threshold of paroxysmal to persistent AF, rather than patients with already persistent AF.

Another potential limitation could result from interactions between atrial electrophysiology, doxapram treatment, respiratory rate, blood pressure, or sympathoadrenergic drive. To comprehensively quantify the effects of doxapram on cardiac electrophysiology and to appreciate the role of the autonomic nervous system in the pathophysiology of AF, EP and hemodynamic measurements were performed without complete autonomic blockade. Even though contribution of TASK-1 to fibroblasts appeared limited (Supplementary material online, *Figure S7*), it remains uncertain whether doxapram has an additional beneficial effect on atrial remodelling beyond its primary electrical effects through modulation of atrial inflammation via TASK-1 channel inhibition in immunocytes or through interaction of central nervous TASK-1 channels. Due to regulations on animal protection, the treatment duration of 14 days was relatively short and sample sizes used in this study were relatively small.

AV node ablation was performed in the AF group to prevent tachycardiomyopathy because left ventricular ejection fraction was identified as an important remote regulator of atrial TASK-1 currents.[8] Rapid conduction through the AV node is, however, part and parcel of atrial arrhythmogenesis in patients with heart failure. It has to be taken into account that this element of the clinical picture of AF is not taken into consideration in the animal model that was used in this study. It further has to be acknowledged that not all study groups underwent AV node

ablation, as we aimed to assess the effects of doxapram on AV nodal conduction.

5. Conclusion

Pharmacological suppression of atrial TASK-1 potassium channels prolonged atrial refractoriness with no effects on ventricular repolarization, resulting in atrial-specific class-III antiarrhythmic effects. In our preclinical pilot study using a clinically relevant large animal model, the respiratory stimulant doxapram was successfully administered for cardioversion of acute episodes of paroxysmal AF as well as rhythm control of persistent AF. Further clinical trials are needed to evaluate the effects of doxapram in AF patients. Finally, experiments of this study served as the basis for preparing the first clinical trial of a TASK-1 inhibitor in AF patients, the DOCTOS trial, to convert AF.

Supplementary material

Supplementary material is available at *Cardiovascular Research* online.

Authors' contributions

F.W. and C.S. designed, performed, and analysed the majority of experiments in this study and co-wrote the manuscript. N.D., G.v.L., and S.K. provided valuable support on experimental design, data analysis, and interpretation. C.B., F.W., M.Kr., and C.S. performed the large animal experiments. F.W., M.Kr., N.J., A.P., S.R., and A.Bü. performed and analysed the two electrode voltage–clamp experiments in *Xenopus laevis* oocytes and patch-clamp experiments in human atrial cardiomyocytes. A.Bü. performed and visualized the molecular docking simulations. X.-B.Z., I.E.-B., X.L., S.L., I.A., and M.B. performed patch-clamp experiments in isolated porcine cardiomyocytes. M.Kr., K.I.F., A.Bl., and W.E.H. performed the MS doxapram plasma level analysis. H.S. and J.H. performed the computational simulations. U.T., J.K., R.A., and M.Ka. contributed to human tissue sample acquisition. M.Ka., N.D., G.v.L., M.B., S.K., J.H., W.E.H., and H.A.K. supported manuscript and figure preparation. C.S. supervised the project. All authors have approved the submitted version of the manuscript and have agreed to be personally accountable for their contributions.

Acknowledgements

We thank Sabine Höllriegel, Patricia Kraft, Katrin Kupser, and Lisa Künstler for excellent technical support.

Conflict of interest: F.W., H.A.K., and C.S. have filed a patent application for *KCNK3*-based gene therapy for cardiac arrhythmia. F.W., N.D., W.E.H, H.A.K., and C.S. have filed a patent application for pharmacological TASK-1 inhibition in treatment of atrial arrhythmia. The remaining authors have reported that they have no relationships relevant to the content of this article to disclose.

Funding

This work was supported by research grants from the University of Heidelberg, Faculty of Medicine, Heidelberg, Germany [Rahel Goitein-Straus Scholarship and Olympia-Morata Scholarship to C.S.]; the German Center for Cardiovascular Research, Berlin, Germany (DZHK) [Excellence Grant to C.S.; Excellence Program: Postdoc Start-up Grant to F.W.]; the German Cardiac Society (DGK), Dusseldorf, Germany [Research Scholarship DGK082018 to F.W.; Otto-Hess Fellowship to F.W. and C.B.]; the German Heart Foundation/German Foundation of Heart Research, Frankfurt [F/15/18 to F.W., F/41/15 to C.S., Kaltenbach Scholarship to A.B. and F.W.]; the Joachim-Herz Foundation, Hamburg, Germany [PostDoc Addon-Fellowship to F.W.] and from the German Research Foundation (DFG), Bonn, Germany [SCHM 3358/1-1 to C.S., SFB 1425 to C.S.].

Data availability

The data underlying this article are available in the article and in its Supplementary material online.

References

1.. January CT, Wann LS, Calkins H, Chen LY, Cigarroa JE, Cleveland JC, Ellinor PT, Ezekowitz MD, Field ME, Furie KL, Heidenreich PA, Murray KT, Shea JB, Tracy CM, Yancy CW. 2019 AHA/ACC/HRS focused update of the 2014 AHA/ACC/HRS guideline for the management of patients with atrial fibrillation: a report of the American College of Cardiology/American Heart Association Task Force on Clinical Practice Guidelines and the Heart Rhythm Society. *J Am Coll Cardiol* 2019;**74**:104–132.

2. Hindricks G, Potpara T, Dagres N, Arbelo E, Bax JJ, Blomström-Lundqvist C, Boriani G, Castella M, Dan G-A, Dilaveris PE, Fauchier L, Filippatos G, Kalman JM, La Meir M, Lane DA, Lebeau JP, Lettino M, Lip GYH, Pinto FJ, Thomas GN, Valgimigli M, Van Gelder IC, Van Putte BP, Watkins CL. 2020 ESC Guidelines for the diagnosis and management of atrial fibrillation developed in collaboration with the European Association for Cardio-Thoracic Surgery (EACTS) The Task Force for the diagnosis and management of atrial fibrillation of the European Society of Cardiology (ESC) Developed with the special contribution of the European Heart Rhythm Association (EHRA) of the ESC. *Eur Heart J* 2021;**42**:373–498.
3. Rahman F, Kwan GF, Benjamin EJ. Global epidemiology of atrial fibrillation. *Nat Rev Cardiol* 2014;**11**:639.
4. Peyronnet R, Ravens U. Atria-selective antiarrhythmic drugs in need of alliance partners. *Pharmacol Res* 2019;**145**:104262.
5. Duprat F, Lesage F, Fink M, Reyes R, Heurteaux C, Lazdunski M. TASK, a human background K^+ channel to sense external pH variations near physiological pH. *EMBO J* 1997;**16**:5464–5471.
6. Goldstein SA, Bockenhauer D, O'Kelly I, Zilberberg N. Potassium leak channels and the *KCNK* family of two-P-domain subunits. *Nat Rev Neurosci* 2001;**2**:175–184.
7. Schmidt C, Wiedmann F, Voigt N, Zhou XB, Heijman J, Lang S, Albert V, Kallenberger S, Ruhparwar A, Szabó G, Kallenbach K, Karck M, Borggrefe M, Biliczki P, Ehrlich JR, Baczkó I, Lugenbiel P, Schweizer PA, Donner BC, Katus HA, Dobrev D, Thomas D. Upregulation of $K_{2P}3.1$ K^+ current causes action potential shortening in patients with chronic atrial fibrillation. *Circulation* 2015;**132**:82–92.
8. Schmidt C, Wiedmann F, Zhou XB, Heijman J, Voigt N, Ratte A, Lang S, Kallenberger SM, Campana C, Weymann A, De SR, Szabo G, Ruhparwar A, Kallenbach K, Karck M, Ehrlich JR, Baczkó I, Borggrefe M, Ravens U, Dobrev D, Katus HA. Thomas D. Inverse remodelling of $K_{2P}3.1$ K^+ channel expression and action potential duration in left ventricular dysfunction and atrial fibrillation: implications for patient-specific antiarrhythmic drug therapy. *Eur Heart J* 2017;**38**:1764–1774.
9. Voigt N, Dobrev D. Ion channel remodelling in atrial fibrillation. *Eur Cardiol* 2011;**7**:97–103.
10. Voigt N, Friedrich A, Bock M, Wettwer E, Christ T, Knaut M, Strasser RH, Ravens U, Dobrev D. Differential phosphorylation-dependent regulation of constitutively active and muscarinic receptor-activated $I_{K,ACh}$ channels in patients with chronic atrial fibrillation. *Cardiovasc Res* 2007;**74**:426–437.
11. Voigt N, Li N, Wang Q, Wang W, Trafford AW, Abu-Taha I, Sun Q, Wieland T, Ravens U, Nattel S, Wehrens XH, Dobrev D. Enhanced sarcoplasmic reticulum Ca^{2+} leak and increased Na^+-Ca^{2+} exchanger function underlie delayed afterdepolarizations in patients with chronic atrial fibrillation. *Circulation* 2012;**125**:2059–2070.
12. Schotten U, Verheule S, Kirchhof P, Goette A. Pathophysiological mechanisms of atrial fibrillation: a translational appraisal. *Physiol Rev* 2011;**91**:265–325.
13. Nattel S, Burstein B, Dobrev D. Atrial remodeling and atrial fibrillation: mechanisms and implications. *Circ Arrhythm Electrophysiol* 2008;**1**:62–73.
14. Putzke C, Wemhöner K, Sachse FB, Rinné S, Schlichthörl G, Li XT, Jaé L, Eckhardt I, Wischmeyer E, Wulf H, Preisig-Müller R, Daut J, Decher N. The acid-sensitive potassium channel TASK-1 in rat cardiac muscle. *Cardiovasc Res* 2007;**75**:59–68.
15. Streit AK, Netter MF, Kempf F, Walecki M, Rinné S, Bollepalli MK, Preisig-Müller R, Renigunta V, Daut J, Baukrowitz T, Sansom MS, Stansfeld PJ, Decher N. A specific two-pore domain potassium channel blocker defines the structure of the TASK-1 open pore. *J Biol Chem* 2011;**286**:13977–13984.

16. Kiper AK, Rinné S, Rolfes C, Ramírez D, Seebohm G, Netter MF, González W, Decher N. Kv1.5 blockers preferentially inhibit TASK-1 channels: TASK-1 as a target against atrial fibrillation and obstructive sleep apnea? *Pflugers Arch* 2015;**467**: 1081–1090.
17. Wiedmann F, Schmidt C, Lugenbiel P, Staudacher I, Rahm AK, Seyler C, Schweizer PA, Katus HA, Thomas D. Therapeutic targeting of two-pore-domain potassium (K_{2P}) channels in the cardiovascular system. *Clin Sci (Lond)* 2016;**130**:643–650.
18. Wiedmann F, Beyersdorf C, Zhou X, Büscher A, Kraft M, Nietfeld J, Walz TP, Unger LA, Loewe A, Schmack B, Ruhparwar A, Karck M, Thomas D, Borggrefe M, Seemann G, Katus HA, Schmidt C. Pharmacologic TWIK-related acid-sensitive K^+ channel (TASK-1) potassium channel inhibitor A293 facilitates acute cardioversion of paroxysmal atrial fibrillation in a porcine large animal model. *J Am Heart Assoc* 2020;**9**: e015751.
19. Wiedmann F, Beyersdorf C, Zhou X-B, Kraft M, Foerster KI, El-Battrawy I, Lang S, Borggrefe M, Haefeli WE, Frey N, Schmidt C. The experimental TASK-1 potassium channel inhibitor A293 can be employed for rhythm control of persistent atrial fibrillation in a translational large animal model. *Front Physiol* 2021;**11**:629421.
20. Cotten JF. TASK-1 (KCNK3) and TASK-3 (KCNK9) tandem pore potassium channel antagonists stimulate breathing in isoflurane-anesthetized rats. *Anesth Analg* 2013; **116**:810–816.
21. Chokshi RH, Larsen AT, Bhayana B, Cotten JF. Breathing stimulant compounds inhibit TASK-3 potassium channel function likely by binding at a common site in the channel pore. *Mol Pharmacol* 2015;**88**:926–934.
22. O'Donohoe PB, Huskens N, Turner PJ, Pandit JJ, Buckler KJ. A1899, PK-THPP, ML365, and Doxapram inhibit endogenous TASK channels and excite calcium signaling in carotid body type-1 cells. *Physiol Rep* 2018;**6**:e13876.
23. Cunningham KP, MacIntyre DE, Mathie A, Veale EL. Effects of the ventilatory stimulant, doxapram on human TASK-3 (KCNK9, K_{2P}9.1) channels and TASK-1 (KCNK3, K_2P3.1) channels. *Acta Physiol (Oxf)* 2020;**228**:e13361.
24. Yost CS. A new look at the respiratory stimulant doxapram. *CNS Drug Rev* 2006;**12**: 236–249.
25. Schmidt C, Wiedmann F, Langer C, Tristram F, Anand P, Wenzel W, Lugenbiel P, Schweizer PA, Katus HA, Thomas D. Cloning, functional characterization, and remodeling of K_{2P}3.1 (TASK-1) potassium channels in a porcine model of atrial fibrillation and heart failure. *Heart Rhythm* 2014;**11**:1798–1805.
26. Rödström KEJ, Kiper AK, Zhang W, Rinné S, Pike ACW, Goldstein M, Conrad LJ, Delbeck M, Hahn MG, Meier H, Platzk M, Quigley A, Speedman D, Shrestha L, Mukhopadhyay SMM, Burgess-Brown NA, Tucker SJ, Müller T, Decher N, Carpenter EP. A lower X-gate in TASK channels traps inhibitors within the vestibule. *Nature* 2020;**582**:443–447.
27. Wiedmann F, Kiper AK, Bedoya M, Ratte A, Rinné S, Kraft M, Waibel M, Anad P, Wenzel W, González W, Katus HA, Decher, N, Schmidt, C. Identification of the A293 (AVE1231) binding site in the cardiac two-pore-domain potassium channel task-1: a common low affinity antiarrhythmic drug binding site. *Cell Physiol Biochem* 2019;**52**:1223–1235.
28. Wiedmann F, Schulte JS, Gomes B, Zafeiriou MP, Ratte A, Rathjens F, Fehrmann E, Scholz B, Voigt N, Müller FU, Thomas D, Katus HA, Schmidt C. Atrial fibrillation and heart failure-associated remodeling of two-pore-domain potassium (K_{2P}) channels in murine disease models: focus on TASK-1. *Basic Res Cardiol* 2018;**113**:27.
29. Schmidt C, Wiedmann F, Beyersdorf C, Zhao Z, El-Battrawy I, Lan H, Szabo G, Li X, Lang S, Korkmaz-Icöz S, Rapti K, Jungmann A, Ratte A, Müller OJ, Karck M, Seemann G, Akin I, Borggrefe M, Zhou XB, Katus HA, Thomas D. Genetic ablation of TASK-1 (tandem of P domains in a weak inward rectifying K^+ channel-related acid-sensitive K^+ channel-1) (K_{2P}3.1) K^+ channels suppresses atrial fibrillation and prevents electrical remodeling. *Circ Arrhythm Electrophysiol* 2019;**12**:e007465.
30. Narula OS, Shantha N, Vasquez M, Towne WD, Linhart JW. A new method for measurement of sinoatrial conduction time. *Circulation* 1978;**58**:706–714.
31. Strauss HC, Saroff AL, Bigger JT Jr, Giardina EG. Premature atrial stimulation as a key to the understanding of sinoatrial conduction in man. Presentation of data and critical review of the literature. *Circulation* 1973;**47**:86–93.
32. Limberg SH, Netter MF, Rolfes C, Rinné S, Schlichthörl G, Zuzarte M, Vassiliou T, Moosdorf R, Wulf H, Daut J, Sachse FB, Decher N. TASK-1 channels may modulate action potential duration of human atrial cardiomyocytes. *Cell Physiol Biochem* 2011; **28**:613–624.
33. Pushpakom S, Iorio F, Eyers PA, Escott KJ, Hopper S, Wells A, Doig A, Guilliams T, Latimer J, McNamee C, Norris A, Sanseau P, Cavalla D, Pirmohamed M. Drug repurposing: progress, challenges and recommendations. *Nat Rev Drug Discov* 2019;**18**: 41–58.
34. Lesage F, Lazdunski M. Molecular and functional properties of two-pore-domain potassium channels. *Am Jour Physiol Renal Physiol* 2000;**279**:F793–F801.
35. Clark RB, Kondo C, Belke DD, Giles WR. Two-pore domain K^+ channels regulate membrane potential of isolated human articular chondrocytes. *J Physiol* 2011;**589**: 5071–5089.
36. Bedoya M, Rinné S, Kiper AK, Decher N, González W, Ramírez D. TASK channels pharmacology: new challenges in drug design. *J Med Chem* 2019;**62**:10044–10058.
37. Davies LA, Hu C, Guagliardo NA, Sen N, Chen X, Talley EM, Carey RM, Bayliss DA, Barrett PQ. TASK channel deletion in mice causes primary hyperaldosteronism. *Proc Natl Acad Sci USA* 2008;**105**:2203–2208.
38. Enyedi P, Czirják G. Molecular background of leak K^+ currents: two-pore domain potassium channels. *Physiol Rev* 2010;**90**:559–605.
39. Meuth SG, Bittner S, Meuth P, Simon OJ, Budde T, Wiendl H. TWIK-related acid-sensitive K^+ channel 1 (TASK1) and TASK3 critically influence T lymphocyte effector functions. *J Biol Chem* 2008;**283**:14559–14570.
40. Kim S, Collins WA, Shoemaker VW. Hemodynamic responses to doxapram in normovolemic and hypovolemic dogs. *Anesth Analg* 1971;**50**:705–710.
41. Laxenaire M, Boileau S, Dagrenat P, Menu N, Drouet N. Haemodynamic and respiratory effects of post-operative doxapram and almitrine in patients following pneumonectomy. *Eur J Anaesthesiol* 1986;**3**:259–271.
42. Conti F, Bertoli L, Bertoli M, Mantero O. Ventilatory and pulmonary hemodynamic response to the respiratory stimulant doxapram in chronic bronchitis. *Pharm Res Com* 1976;**8**:243–251.
43. Olschewski A, Li Y, Tang B, Hanze Jr, Eul B, Bohle RM, Wilhelm J, Morty RE, Brau ME, Weir EK, Kwapiszewska G, Klepetko W, Seeger W, Olschewski H. Impact of TASK-1 in human pulmonary artery smooth muscle cells. *Circ Res* 2006;**98**: 1072–1080.
44. Shimokaze T, Toyoshima K, Shibasaki J, Itani Y. Blood potassium and urine aldosterone after doxapram therapy for preterm infants. *J Perinatol* 2018;**38**:702–707.
45. Fischer C, Ferdynus C, Gouyon J-B, Semama DS. Doxapram and hypokalaemia in very preterm infants. *Arch Dis Child Fetal Neonatal Ed* 2013;**98**:F416–F418.
46. Wasserman AJ, Richardson DW. Human cardiopulmonary effects of doxapram, a respiratory stimulant. *Clin Pharmacol Ther* 1963;**4**:321–325.
47. Maillard C, Boutroy MJ, Fresson J, Barbé F, Hascoët JM. QT interval lengthening in premature infants treated with doxapram. *Clin Pharmacol Ther* 2001;**70**:540–545.
48. Stephen CR, Talton I. Effects of doxapram on the electrocardiogram during anesthesia. *Anesth Analg* 1966;**45**:783–789.
49. De Villiers G, Walele A, Van der Merwe P, Kalis N. Second-degree atrioventricular heart block after doxapram administration. *J Pediatr* 1998;**133**:149–150.
50. Huffington P, Craythorne NW. Effect of doxapram on heart rhythm during anesthesia in dog and man. *Anesth Analg* 1966;**45**:558–563.